

## AUTHOR QUERY FORM

	<b>Journal:</b> Appl. Phys. Lett.	Please provide your responses and any corrections by annotating this PDF and uploading it according to the instructions provided in the proof notification email.
	<b>Article Number:</b> 009738APL	

Dear Author,

Below are the queries associated with your article; please answer all of these queries before sending the proof back to AIP.

**Article checklist:** In order to ensure greater accuracy, please check the following and make all necessary corrections before returning your proof.

1. Is the title of your article accurate and spelled correctly?
2. Please check affiliations including spelling, completeness, and correct linking to authors.
3. Did you remember to include acknowledgment of funding, if required, and is it accurate?

Location in article	Query / Remark: click on the Q link to navigate to the appropriate spot in the proof. There, insert your comments as a PDF annotation.
<a href="#">AQ1</a>	Please check that the author names are in the proper order and spelled correctly. Also, please ensure that each author's given and surnames have been correctly identified (given names are highlighted in red and surnames appear in blue).
<a href="#">AQ2</a>	We were unable to locate a digital object identifier (doi) for Refs. 2 and 3. Please verify and correct author names and journal details (journal title, volume number, page number, and year) as needed and provide the doi. If a doi is not available, no other information is needed from you. For additional information on doi's, please select this link: <a href="http://www.doi.org/">http://www.doi.org/</a> .

Thank you for your assistance.

# 1 Asymmetrically coupled resonators for mass sensing

2 S. Marquez,<sup>1</sup> M. Alvarez,<sup>2,a)</sup> J. A. Plaza,<sup>2</sup> L. G. Villanueva,<sup>3</sup> C. Dominguez,<sup>2</sup>  
3 and L. M. Lechuga<sup>1</sup>

4 <sup>1</sup>Nanobiosensors and Bioanalytical Applications Group, Catalan Institute of Nanoscience and Nanotechnology  
5 (ICN2), CSIC and The Barcelona Institute of Science and Technology, CIBER-BBN, Campus UAB, Bellaterra,  
6 Spain

7 <sup>2</sup>Instituto de Microelectrónica de Barcelona (IMB-CNM, CSIC), Campus UAB, Bellaterra, Spain

8 <sup>3</sup>Advanced NEMS Group, École Polytechnique Fédérale de Lausanne (EPFL), CH-1015 Lausanne,  
9 Switzerland

10 (Received 21 March 2017; accepted 1 September 2017; published online xx xx xxxx)

11 Mechanically coupled resonators have been applied in the last years to the development of  
12 nanomechanical mass-sensors based on the detection of the different vibration modes of the system  
13 by measuring on a single resonator. Their sensitivity and capability for detecting multiple analytes  
14 strongly depends on the design and coupling strength between the mechanically coupled resonators  
15 in an array format. We present a theoretical and experimental study of the behavior of an asymmet-  
16 rically coupled array of four different resonators. These doubly clamped beam resonators are elasti-  
17 cally coupled by an overhang region of varying length along the transversal axis of the array. The  
18 results show that parameters such as the gap between microbeams and the overhang length affect  
19 the coupling strength, tuning the system from highly disordered and highly localized (weak cou-  
20 pling) to highly delocalized (strong coupling). In the strong coupling and partially localized case,  
21 the distances between resonant peaks are larger, reaching higher eigenfrequency values. In this  
22 case, relative changes in a specific eigenstate, due to an added mass, can be markedly large due to  
23 the energy distribution over a single microbeam. A strong coupling also facilitates performing the  
24 detection on the relative frequency shift mode, which can usually be resolved with better precision  
25 than the amplitude changes. *Published by AIP Publishing.* [<http://dx.doi.org/10.1063/1.5003023>]

26 One of the key features sought when developing a mass  
27 sensor is the capability to simultaneously detect several analy-  
28 tes. In the case of microcantilevers or microbeams based bio-  
29 sensors, the development of a high-throughput system  
30 involves not only the fabrication of arrays of microcantilevers,  
31 which is currently a well-established and low-cost process,  
32 but also the implementation of a complex read-out system to  
33 independently read each microcantilever response.<sup>1-3</sup>

34 The use of mechanically coupled resonators arises as an  
35 alternative to avoid this drawback, by allowing the detection  
36 of several resonators using a single input and single output  
37 approach.<sup>4,5</sup> The mechanical coupling of an array of resona-  
38 tors to a common mass produces a mode localization phenom-  
39 enon. An action on any of the resonators affects the vibration  
40 state of the other resonators. When adding a perturbation (e.g.,  
41 a mass) to the coupled resonators, the periodicity of the sys-  
42 tem is broken, changing the dynamics of the structure and  
43 leading to the localization of the vibration energy at certain  
44 areas of the system (Anderson's localization).<sup>6</sup>

45 Coupled systems present several resonance peaks where  
46 each peak is related to a specific mode of the coupled system.  
47 The resonant peaks of the coupled system expand depending  
48 on the stiffness of the coupling region between resonators,  $k_c$ .  
49 For periodic, four identical mechanically coupled resonators,  
50 with identical stiffness  $k$  and effective mass  $m$ , the minimum  
51 resonance frequency corresponds to the an isolated oscillator,

while the maximum resonance frequency increases with the  
strength of the coupling,<sup>7</sup> as shown in the below equation

$$\omega_1 = \sqrt{\frac{k}{m}},$$

$$\omega_4 = \omega_1 \sqrt{1 + 4\kappa}, \quad (1)$$

54 where  $\kappa$  is the coupling coefficient, defined as the ratio of  
55 stiffness of the coupling element to the stiffness of the reso-  
56 nating element,  $\kappa = k_c/k$ . In the scope of this work, weak  
57 coupling is defined when  $\kappa < 0.05$ , while strong coupling is  
58 when  $\kappa \geq 0.05$ . When the coupled resonators are nearly  
59 identical, the eigenstates are said to be non-localized, and  
60 beautiful examples of collective dynamics can be found in  
61 the literature,<sup>8-11</sup> and start becoming localized when a small  
62 mass is added to one of the resonators (in each eigenstate,  
63 one resonator oscillates more than the other).<sup>12,13</sup> By  
64 decreasing the mechanical coupling coefficient, the relative  
65 changes between eigenstates (i.e., the normalized mode) can  
66 be larger than the relative change between the eigenvalues of  
67 a single resonator.<sup>7,14</sup> When such a strong localization  
68 occurs, the effect of the added mass causes a drastic change  
69 in the system dynamics,<sup>15</sup> enhancing the amplitude  
70 changes.<sup>16,17</sup> Working with an array of 15 nearly identical  
71 coupled microcantilevers, Spletzer *et al.* propose the exami-  
72 nation of experimentally measured patterns of eigenmode  
73 shifts to identify which microcantilever is detecting the ana-  
74 lyte.<sup>13</sup> Lee *et al.* demonstrate the feasibility of performing  
75 quantitative photoacoustic spectroscopy with six identical  
76 microcantilevers coupled to a shuttle mass.<sup>18</sup> However,

<sup>a)</sup>Author to whom correspondence should be addressed: mar.alvarez@imb-cnm.csic.es

77 although reducing the coupling would increase the respon-  
 78 sivity in a weakly coupled system, this would only work for  
 79 small initial detuning of the individual frequencies. After  
 80 some mass deposition, the system would lose the collective  
 81 behavior and pass to be completely localized, being unusable  
 82 for further sensing. Insertion of asymmetry or non-identical  
 83 resonators in a coupled system provides a method with  
 84 unique responses when any of the resonators is perturbed. In  
 85 this way, DeMartini *et al.* demonstrate single input-single  
 86 output multianalyte detection and identification, by measur-  
 87 ing the resonance frequency variation of a coupled system  
 88 that is strongly localized initially.<sup>19,20</sup> More recently, the sig-  
 89 nal-to-noise ratio amplification of strong coupled systems  
 90 has been as well demonstrated.<sup>21</sup>

91 In this work, we make use of mechanically coupled  
 92 resonators for implementing a system able to detect several  
 93 analytes simultaneously, reducing the required read-out  
 94 instrumentation and simplifying the data processing, while  
 95 maintaining a high sensitivity and dynamic range. To that  
 96 end, we propose an original geometry of four dissimilar fre-  
 97 quency resonators with different (asymmetric) mechanical  
 98 coupling between neighboring resonators to modulate the  
 99 coupled system response. We investigate the effect of the  
 100 coupling strength on the performance of such a system  
 101 experimentally and numerically by using finite element anal-  
 102 ysis (FEA).

103 The proposed mechanical sensor is composed of an  
 104 array of four microbeams clamped at both ends by an over-  
 105 hang region of varying length along the array. To achieve  
 106 this, the set of microbeams is fabricated inside a trapezoidal  
 107 frame, with a specific slope on two of the sides, as shown in  
 108 Fig. 1(a), which leads to microbeams with small variations  
 109 in their lengths and, therefore, in their natural individual  
 110 non-coupled resonance frequencies. At the same time, the  
 111 coupling stiffness ratio,  $\kappa = k_{c,i}/k_{b,i}$  (with  $k_{c,i}$  being the cou-  
 112 pling region spring constant and  $k_{b,i}$  being the beam spring  
 113 constant), is different between neighboring resonators, being  
 114 lower for beams with smaller overhang length.<sup>14</sup> Different  
 115 combinations of the frame slope, the gap between microbe-  
 116 ams and the microbeam widths are analyzed. The proposed  
 117 system can be considered initially disordered in the sense  
 118 that all the resonators have different individual natural  
 119 frequencies.

120 The mechanical sensor is fabricated following a process  
 121 that is described in detail in the [supplementary material](#) (Fig.  
 122 S1). We fabricate various different arrays of four doubly  
 123 clamped beam resonators into 300  $\mu\text{m}$  length frames. We  
 124 sweep three parameters in the design: slope angle of the cou-  
 125 pling region ( $3^\circ$ ,  $5^\circ$ , and  $7^\circ$ ), beam width ( $w = 10 \mu\text{m}$ ,  $20 \mu\text{m}$ ,  
 126 and  $35 \mu\text{m}$ ), and inter-beam gap ( $g = 10 \mu\text{m}$  and  $20 \mu\text{m}$ ), for a  
 127 total of 18 different designs. The thickness of the beams is  
 128  $2 \mu\text{m}$ . Silicon nitride and silicon oxide are the microbeams  
 129 main structural material. We achieve the coupling ledge, see  
 130 Figs. 1(a) and 1(b), in silicon nitride by over-etching during  
 131 release with 25% Tetramethylammonium Hydroxide (TMAH).

132 The characterization of these devices is performed using  
 133 an in-house free-space optical interferometer, locating the  
 134 laser spot approximately in the middle of each beam. The  
 135 frequency spectra are obtained by performing a Fast Fourier  
 136 Transform (FFT) of the thermomechanical noise response of

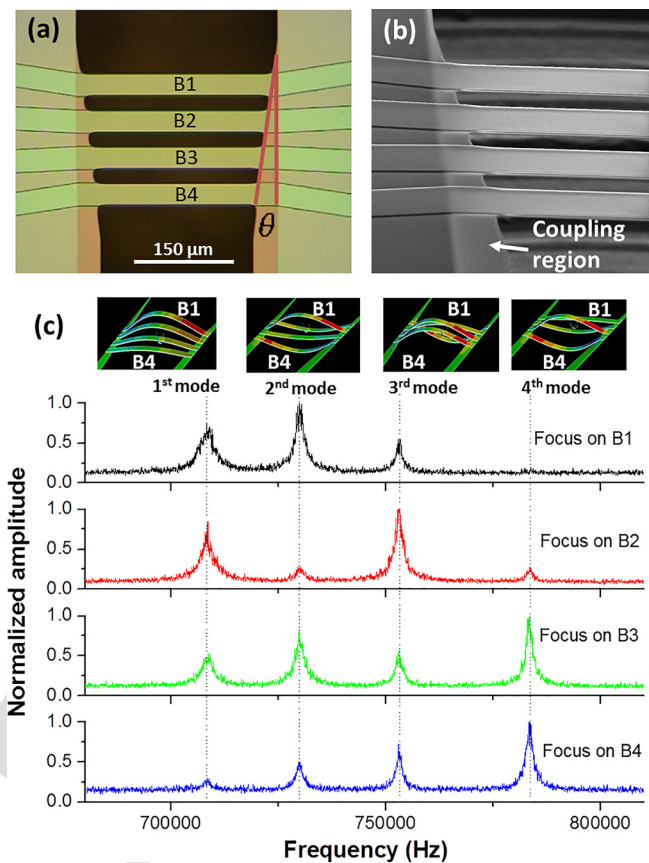


FIG. 1. Image of the fabricated coupled array structure: (a) under the optical microscope and (b) under SEM. (c) Modal analysis of the first four eigenstates obtained by FEA, and experimental resonance spectra when focusing on the middle of each microbeam.

137 the array. Using the Brownian motion of the devices ensures  
 138 that the response of the system is spatially uncorrelated.<sup>22</sup> To  
 139 simplify the analysis and discussion within this paper, all  
 140 amplitudes are normalized to the maximum value that is  
 141 obtained in each measurement. Figure 1(c) shows the fre-  
 142 quency spectra for an array configuration of four microbe-  
 143 ams of  $10 \mu\text{m}$  width,  $10 \mu\text{m}$  gap and slope of  $7^\circ$ . The peaks  
 144 in the spectra correspond to the first four eigenstates of the  
 145 coupled system. As expected from theory,<sup>23</sup> the relative  
 146 vibration amplitude of each mode depends on the geometry  
 147 of the whole array but also on the beam on which the mea-  
 148 surement is done.

149 Finite element simulations of the system indicate that  
 150 the lowest resonance peak in the frequency spectrum corre-  
 151 sponds to an eigenstate where all the resonators move in-  
 152 phase [see Fig. 1(c)]. The next three eigenstates of the struc-  
 153 ture correspond to the out-of-plane vibration modes where  
 154 one of the microbeams moves out of phase.

155 The position of the individual modes within the coupled  
 156 system strongly depends on the coupling coefficient,  $\kappa$ , which  
 157 varies with the coupling region geometry. An increase in the  
 158 length of the coupling region (i.e., higher slopes), facilitates  
 159 the distribution of the energy in the coupled system, inducing  
 160 a more delocalized response of the vibration modes (strong  
 161 coupling). Consequently, the separation of the frequency  
 162 peaks augments, facilitating the identification of each eigen-  
 163 state. This is confirmed experimentally for systems of mini-  
 164 mum beam width and gap ( $g = 10 \mu\text{m}$ ,  $w = 10 \mu\text{m}$ ), where the

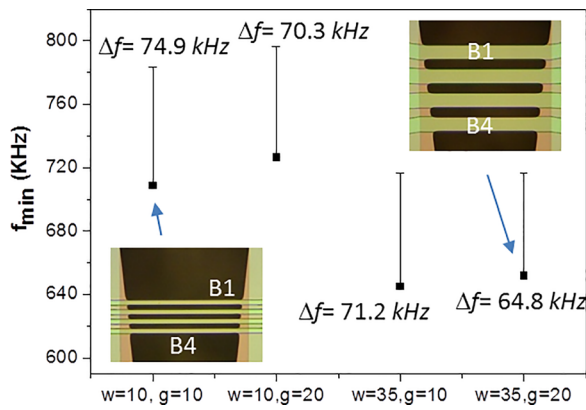


FIG. 2. Effect of the microbeam width and gap on the minimum resonant frequency of the system (bars representing the frequency splitting, the distance between maximum and minimum frequency), for a frame slope of 7°.

165 coupling between resonators increases for higher slopes (see  
 166 Fig. S2 in the [supplementary material](#)). The system eigenfre-  
 167 quencies overlap for the case of a slope of 3° which presents a  
 168 narrow frequency splitting ( $\Delta f = 20$  kHz) and the lower cou-  
 169 pling coefficient estimated from Eq. (1) ( $\kappa = 0.015$ ). The total  
 170 splitting increases with the slope angle, attaining values of  
 171  $\Delta f = 43$  kHz for 5° and  $\Delta f = 74$  kHz for 7°. Increasing the  
 172 slope angle and reducing the gap<sup>14</sup> provide the largest splitting  
 173 (strongest coupling,  $\kappa > 0.05$ ).

174 For a given slope, the coupling between resonators  
 175 decreases when the gap of the microbeams increase, as  
 176 shown in Fig. 2 for a slope of 7°. As expected, the response  
 177 of arrays with narrower microbeams occurs at higher fre-  
 178 quencies and with larger frequency splitting. Similarly,  
 179 arrays with smaller inter-beam gaps show larger frequency  
 180 splitting because of the stronger coupling.

181 Finite element modelling for different geometries repro-  
 182 duces the experimental behavior described in the previous  
 183 paragraph (Fig. 3). When the slope of the ledge is the small-  
 184 est, the coupling is also the smallest, and the system is disor-  
 185 dered and weakly coupled, with the eigenstates localized in  
 186 each individual beam for each vibration mode. In the case of  
 187 an angle of 5°, only the first mode is totally localized, while  
 188 the second, third, and fourth eigenstates are non-localized.  
 189 Finally, the system would be strongly coupled, with all the  
 190 microbeams vibrating in all the system modes, for an angle  
 191 of 7°, 10 μm width and 20 μm gap.

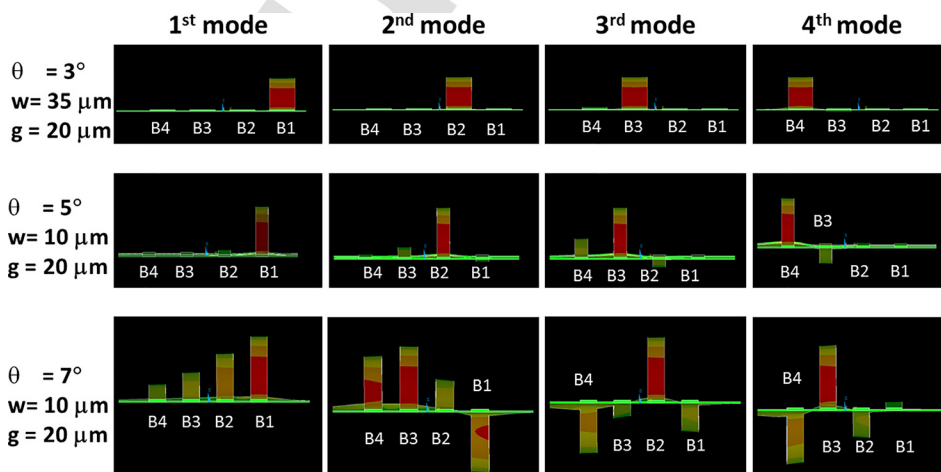


FIG. 3. Finite element modelling of the shape-mode for different array configurations (from weak-coupled and highly localized, to strong-coupled and highly delocalized).

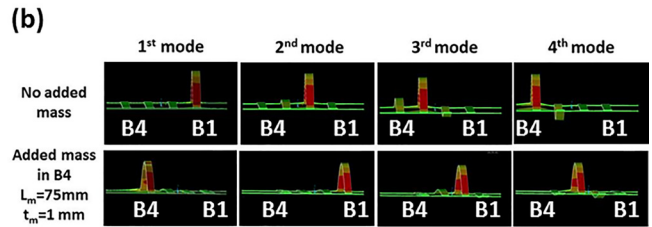
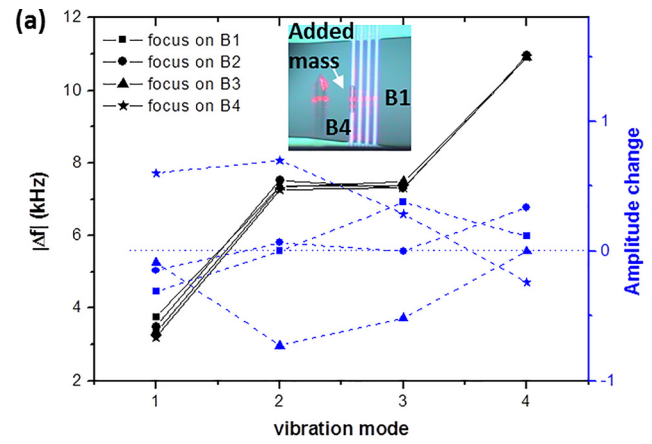


FIG. 4. (a) Experimentally measured frequency and amplitude changes after adding a mass onto the B4 of a coupled array of microbeams with 10 μm width, gap of 10 μm and tilt angle of 5°. (b) Finite element simulations results for the same array configuration before and after adding a homogeneous mass of  $75 \times 10 \times 1 \mu\text{m}^3$  on the center of the fourth beam.

Depending on the strength of coupling and the magni- 192  
 tude of disorder, upon mass addition the vibration energy 193  
 localizes more in certain beams of the structure. Adding a 194  
 mass to one of the beams tends to localize more the vibration 195  
 around the loaded beam at lower frequencies. If sufficient 196  
 mass is added, the eigenstate with the lowest frequency cor- 197  
 responds to a vibration of the beam where the mass was 198  
 added, and that alone. 199

In order to experimentally evaluate the effect of mass 200  
 change over the system, we deposit a volume of a thermally 201  
 killed bacteria (*Listeria*) solution 10 nM (in SSC 5× buffer) 202  
 by using a drop deposition system able to print spots down to 203  
 10 μm (NanoEnabler system, Bioforce, USA). The printed 204  
 volume is deposited at the middle of a beam [in the case 205  
 shown in Fig. 4(a), this is beam B4] to maximize the effect 206  
 of the mass change with respect to that of the stiffness 207  
 change (which is higher when the load is added near the 208

TABLE I. Comparison of the simulated,  $F_{\text{sim}}$ , and measured,  $F_{\text{exp}}$ , eigenvalues (kHz), before and after adding a mass.

	F exp.	F sim.	F mass exp.	F mass sim.
Peak 1	699.08	711.45	695.89	693.04
Peak 2	710.62	715.92	703.36	709.08
Peak 3	723.03	721.32	715.71	714.32
Peak 4	742.30	731.12	731.37	720.85

clamped ends).<sup>24</sup> The volume is then dried before the measurement to stick it to the beam.

Figure 4(a) shows the largest frequency change (before/after mass addition) on the fourth eigenstate, which is consistent with the finite element modelling results. As expected, the observed frequency shift does not depend on the beam where we perform the measurement, other than a slight shift due to warming up of the beam.<sup>25</sup> The mass responsivity of the  $i$ th mode is defined as  $\mathfrak{R} \approx \Delta f_i / \Delta m_{\text{eff}}$ , where  $m_{\text{eff}}$  is the mode effective mass.

Figure 4(a) also shows the change in vibration amplitude, i.e., change in the eigenmodes. In this case, we can evidently see a strong variation depending on the beam where we focus the laser spot. Zero amplitude change indicates that the amplitude of the mode does not change after adding the mass. It also shows that, while the effect of adding the mass is certainly measurable, it is different depending on the modes, and may even be opposite for certain modes in this strongly coupled asymmetric system (see also Fig. S3 in the supplementary material). This suggests that a detection method based on frequency shifts may be more adequate when using strongly coupled arrays,<sup>26</sup> as opposed to the mainstream thought of using amplitude measurements.<sup>12</sup>

Figure 4(b) shows the results of finite element simulations when a mass that covers a whole central area of the B4 beam is added. The simulations show that the main effect of adding the mass is to concentrate the energy of the first mode on the microbeam being loaded, which agrees with the experimental observations, where the energy of the system is redistributed towards the first vibration mode when focusing on B4. Further simulations in which the load is applied to different beams confirm this point (see Fig. S4 in the supplementary material).

The dimensions, density, and location of the added mass, as well as the pre-stress magnitude, are chosen in the simulation (within a realistic boundaries) to match the experimentally measured frequencies (see Table I). One possible cause of discrepancies between experimentally measured and simulated frequency values is the local variations in dimensions and properties (e.g., the simulations assumed homogeneous pre-stress for the whole array).

In conclusion, we discuss the interplay of different parameters on the coupling strength of different length asymmetrically coupled resonators. Various geometries are studied ranging from highly localized (weak coupling) to highly delocalized (strong coupling) systems. The results show the effect of the design on the final sensitivity of the system for mass sensing. With the proposed design, if sufficient mass is added into a beam, the eigenstate with the lowest frequency corresponds to a vibration of the beam where the mass is

added. This makes it possible to identify the beam reacting during a biodetection by measuring the mode amplitude change. Also, a strong coupling facilitates performing the detection on the relative frequency shift mode which can usually be resolved with better precision than the amplitude changes.

See supplementary material for detailed information about the fabrication process and additional graphs of the system behavior (experimental and simulated) is available.

The authors acknowledge the financial support from National Council for Science and Technology (CONACyT-Mexico); from the Ministerio de Economía y Competitividad (MINECO) (Spain) through Ramon y Cajal program (RYC-2013-14479) and MINAHE 5 MINECO/ICTI 2013-2016/TEC2014-51940-C2 and by the EU ERDF (FEDER) funds; and from the Swiss National Science Foundation (PP00P2-144695). Fabrication of devices was done at the Spanish ICTS Network MICRONANOFABS partially supported by MINECO under Project No. NGG-244 (GICSERV program). The authors also acknowledge C. Pascual-Izarra for the discussion and revision.

<sup>1</sup>A. Alodhayb, S. M. S. Rahman, S. Rahman, P. E. Georghiou, and L. Y. Beaulieu, *Sens. Actuators, B* **237**, 459 (2016).

<sup>2</sup>N. Maloney, G. Lukacs, N. Nugaeva, W. Grange, J. P. Ramseyer, J. Jensen, and M. Hegner, *J. Sens.* **2012**, e405281 (2011).

<sup>3</sup>M. Alvarez and J. Tamayo, *Sens. Actuators, B* **106**, 687 (2005).

<sup>4</sup>A. A. Glean, J. A. Judge, J. F. Vignola, and T. J. Ryan, *J. Appl. Phys.* **117**, 054505 (2015).

<sup>5</sup>S. Stassi, A. Chiadò, G. Calafiore, G. Palmara, S. Cabrini, and C. Ricciardi, *Sci. Rep.* **7**, 1065 (2017).

<sup>6</sup>P. W. Anderson, *Phys. Rev.* **109**, 1492 (1958).

<sup>7</sup>P. Thiruvengathanathan, J. Woodhouse, J. Yan, and A. A. Seshia, *J. Appl. Phys.* **109**, 104903 (2011).

<sup>8</sup>Q. Chen, L. Huang, and Y.-C. Lai, *Appl. Phys. Lett.* **92**, 241914 (2008).

<sup>9</sup>R. Lifshitz and M. C. Cross, *Phys. Rev. B* **67**, 134302 (2003).

<sup>10</sup>R. B. Karabalin, M. C. Cross, and M. L. Roukes, *Phys. Rev. B* **79**, 165309 (2009).

<sup>11</sup>E. Kenig, M. C. Cross, R. Lifshitz, R. B. Karabalin, L. G. Villanueva, M. H. Matheny, and M. L. Roukes, *Phys. Rev. Lett.* **108**, 264102 (2012).

<sup>12</sup>M. Spletzer, A. Raman, A. Q. Wu, X. Xu, and R. Reifengerber, *Appl. Phys. Lett.* **88**, 254102 (2006).

<sup>13</sup>M. Spletzer, A. Raman, H. Sumali, and J. P. Sullivan, *Appl. Phys. Lett.* **92**, 114102 (2008).

<sup>14</sup>E. Gil-Santos, D. Ramos, V. Pini, M. Calleja, and J. Tamayo, *Appl. Phys. Lett.* **98**, 123108 (2011).

<sup>15</sup>C. Pierre and E. H. Dowell, *J. Sound Vib.* **114**, 549 (1987).

<sup>16</sup>D. Endo, H. Yabuno, K. Higashino, Y. Yamamoto, and S. Matsumoto, *Appl. Phys. Lett.* **106**, 223105 (2015).

<sup>17</sup>D. F. Wang, X. Li, X. Yang, T. Ikehara, and R. Maeda, *J. Microeng. Microeng.* **25**, 095017 (2015).

<sup>18</sup>D. Lee, S. Kim, C. W. V. Neste, M. Lee, S. Jeon, and T. Thundat, *Nanotechnology* **25**, 035501 (2014).

<sup>19</sup>B. E. DeMartini, J. F. Rhoads, S. W. Shaw, and K. L. Turner, *Sens. Actuators, A* **137**, 147 (2007).

<sup>20</sup>B. E. DeMartini, J. F. Rhoads, M. A. Zielke, K. G. Owen, S. W. Shaw, and K. L. Turner, *Appl. Phys. Lett.* **93**, 054102 (2008).

<sup>21</sup>S. Ilyas, N. Jaber, and M. I. Younis, *J. Microelectromech. Syst.* **25**, 916 (2016).

<sup>22</sup>E. Gil-Santos, D. Ramos, A. Jana, M. Calleja, A. Raman, and J. Tamayo, *Nano Lett.* **9**, 4122 (2009).

<sup>23</sup>R. B. Karabalin, Ph.D. dissertation (Caltech, 2008).

<sup>24</sup>K. Zhang, Y. Chai, and J. Fu, *AIP Adv.* **5**, 127109 (2015).

<sup>25</sup>T. Larsen, S. Schmid, L. G. Villanueva, and A. Boisen, *ACS Nano* **7**, 6188 (2013).

<sup>26</sup>M. S. Hajhashemi, A. Rasouli, and B. Bahreyni, *J. Microelectromech. Syst.* **25**, 52 (2016).



AQ2